Eur. Phys. J. D **26**, 47–50 (2003)
DOI: 10.1140/epjd/e2003-00083-y

THE EUROPEAN PHYSICAL JOURNAL D

Optimization of the focused flux of high harmonics

S. Kazamias[1,a], D. Douillet[1], C. Valentin[1], Th. Lefrou[1], G. Grillon[1], G. Mullot[1], F. Augé[1], P. Mercère[1,2], Ph. Zeitoun[1,2], and Ph. Balcou[1]

[1] Laboratoire d'Optique Appliquée, ENSTA-École Polytechnique[b], 91761 Palaiseau Cedex, France
[2] Laboratoire d'Interaction du rayonnement X avec la Matière, bâtiment 350, Université Paris-Sud, 91405 Orsay Cedex, France

Received 15 November 2002 / Received in final form 28 January 2003
Published online 24 April 2003 –

Abstract. Following the theoretical predictions [1], the observation of two-photon processes by interaction of vacuum ultraviolet (VUV) radiation with inner-shell levels of atoms requires focused intensities in the $10^{13}-10^{14}$ W/cm^2 range. Our aim is to reach this regime in order to study non-linear optics at these wavelengths. We first optimized the high harmonic conversion efficiency in argon by studying the best experimental conditions for phase-matching, concentrating on focus geometry related to laser energy, cell length and position relative to the focus. We then studied the resulting harmonic beam focusability by a toroidal mirror ($f = 10$ cm) and made an image of the harmonic focus. We conclude with an evaluation of the focused intensity that we are able to reach experimentally.

PACS. 32.80.Rm Multiphoton ionization and excitation to highly excited states (e.g., Rydberg states) – 42.65.Ky Frequency conversion; harmonic generation, including higher-order harmonic generation

1 Introduction

The potential applications of high focused intensities in the XUV wavelength range are various and quite exciting. Some of them have been already demonstrated, such as two-or even three-photon ionization of rare gases [2,3]. In the near future, VUV ablation by focusing harmonic beams on solid targets is realistic. Optimizing the focused intensity means at the same time optimizing the harmonic energy in the beam and reducing the pulse duration and focus size. This work is thus divided into two parts: in the first one, we explain how we were able to demonstrate high harmonic conversion efficiency in argon around 30 nm by loosely focusing the infrared laser in a gas cell. In the second part, we present a complete study of the focusing of high harmonics. By imaging the focal spots, we can evaluate how much energy we can concentrate on the central spot, leading to a realistic value of the intensity.

2 Optimization of the harmonic flux in the loose focusing geometry

Very recently, different teams in France [4] and one in Japan [5], demonstrated that the use of energetic infrared lasers leads to high number of harmonic photons. High pump energy allows a very loose focusing geometry (5 meter focal length for respectively 27 mJ and 50 mJ) and guarantees an homogeneous phase-matching. Our optimization of high harmonic conversion efficiency in the same focusing conditions ($f/100$) [6] led to comparable values as references [4,5] especially in argon. Our infrared laser installation for high harmonic generation delivers 6 mJ energy in 30 fs at 1 kHz repetition rate. We generate high harmonics in a gas cell and focus the beam with a 1 meter focal length lens. We nevertheless reach the loose focusing geometry by aperturing down the beam to 11 mm diameter whereas the infrared laser initial diameter is 22 mm. In these conditions the Rayleigh range achieved is 17 mm and is much greater than the cell length. The experimental setup is more extensively described in [7].

2.1 Conversion efficiency optimization by aperturing the beam at various laser energies

The importance of the laser energy on optimizing the conversion efficiency by aperturing the beam has been extensively studied. The results are presented in Figure 1, that shows the harmonic signal variation *versus* the size of an iris placed on the infrared beam just before it is focused.

The lower the pump energy is, the higher the optimum aperture is and the smaller the focus longitudinal size (the Rayleigh range is usually called z_0), resulting in smaller harmonic flux. The important thing here, is that aperturing the beam considerably reduces the infrared focused intensity, *via* the iris transmission and the focusing geometry. The cutoff law implies a minimum intensity for

[a] e-mail: kazamias@ensta.fr
[b] CNRS UMR 7639

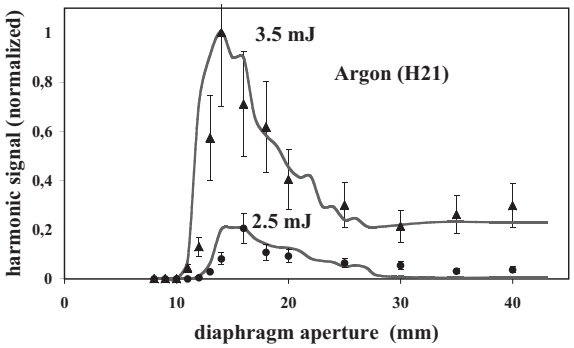

Fig. 1. Comparisons of the harmonic signal as a function of aperture size, for different laser incident energies. Triangles and circles: experimental harmonic signals for the 21st harmonic in argon as a function of diaphragm aperture, with respectively 3.5 mJ and 2.5 mJ total laser energy. Thick line: theoretical simulations with the same generation conditions (15 torr, 5 mm long cell, focus 8 mm before the cell entrance).

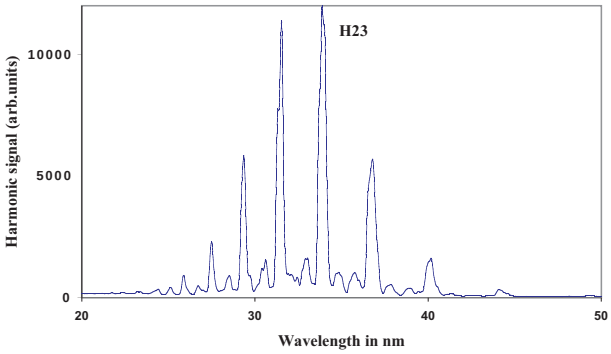

Fig. 2. Harmonic spectrum obtained in optimizing conditions in argon (30 torr, 2 mm long cell, focus 5 mm before the entrance, 6 mJ incident laser energy and 11 mm iris aperture).

a given harmonic to be in the plateau region [8], so that reducing the incident energy means that the optimum iris aperture will be higher. For small laser energies, we are no more in the very loose focusing geometry ($z_0 = 7$ mm) and the conversion efficiency drops to 10^{-6} for the 23rd harmonic order in argon for 3.5 mJ incident energy (see Fig. 1) whereas it was 3×10^{-5} for full laser energy (6 mJ), the resulting spectrum is shown in Figure 2.

A careful calibration of the spectrometer leads to 10^{10} absolute number of photons per shot in the 23rd order, and 3.5×10^{10} photons in the whole spectrum. The total energy is 0.2 μJ and the average power is 0.2 mW. Considering the instantaneous power would lead to much higher value due to the small pulse duration of harmonic. This conversion efficiency is comparable to the value of reference [5] but is 10 times larger than the conversion efficiency recently obtained in argon around 30 nm using a hollow-core-wave-guide geometry, known to be very efficient for phase-matching [10]. A one dimensional phase-matching study in the loose focusing geometry allows us to explain this discrepancy.

2.2 One dimensional time dependent phase-matching study: general frame

In the spirit of reference [9], the harmonic instantaneous flux can be expressed as the product of the microscopic response (atomic polarization) and the macroscopic response of the gas medium characterized by the phase-matching factor F. We define F as the following:

$$F = \frac{1}{1 + 4\pi^2 \frac{l_{\rm abs}^2}{l_{\rm coh}^2}} \left(1 + \mathrm{e}^{\frac{-l_{\rm med}}{l_{\rm abs}}} - 2\cos\left(\pi \frac{l_{\rm med}}{l_{\rm coh}}\right) \mathrm{e}^{\frac{-l_{\rm med}}{2l_{\rm abs}}}\right), \quad (1)$$

where $l_{\rm abs}$ is the absorption length, $l_{\rm coh}$ the coherence length, $l_{\rm med}$ the cell length.

Within this definition, F is a non-dimensional factor between 0 and 1: F equal to 1 means absorption-limited conditions for harmonic generation. This factor is time dependent through the variation of the dispersion and atomic phase gradient terms, whereas the influence of the geometric Gouy phase is constant over the pulse duration. In the one-dimensional approximation, the calculation of the phase matching factor and atomic polarization is possible considering the commonly used ADK ionization rates [11].

2.3 The importance of cell position relative to the focus

Considering the absorption limit, the only way to increase the conversion efficiency is to enhance the atomic response at the time of phase-matching. One can play with the atomic phase gradient whose contribution to phase-matching changes sign at the laser focus. The harmonic generation is indeed known to be produced by the interference between two main quantum paths, each of them is characterized by a specific phase that scales linearly with laser intensity ($\phi = -10^{-14} I(\mathrm{W/cm^2})$ and $-25 \times 10^{-14} I(\mathrm{W/cm^2})$ respectively for the first and second quantum path) [12]. The atomic phase gradient will induce a dispersion term depending on the sign of laser intensity gradient, so that the dispersion will be positive only if the cell is placed after the focus [13].

Figure 3 shows in this condition the time dependence of the one-dimensional phase-matching factor for the two quantum paths. It is clear that $F = 1$ is obtained later in the pulse for the second quantum path, allowing for a better atomic polarization. We thus observed a better harmonic signal for a cell placed after the focus. This result is only valid for loose focusing geometry, whereas for stronger focusing the phase-matching is obtained off-axis when the cell is placed before the focus [14].

2.4 Homogeneity of phase-matching

The main importance of the loose focusing geometry is stressed in Figure 4. We represent the dephasing ϕ between harmonic radiation and laser-induced polarization

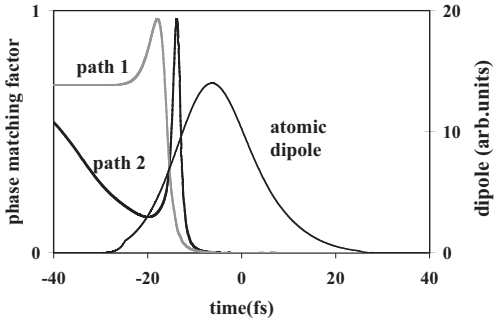

Fig. 3. Time dependence of the phase matching factors associated to the two main quantum paths; grey line: first quantum path, black line: second quantum path, thin line: atomic dipole in arbitrary units (H23 in argon, 20 torr, iris 11 mm, $I = 3 \times 10^{14}$ W/cm^2 at $t = 50$ fs, $z_0 = 8$ mm).

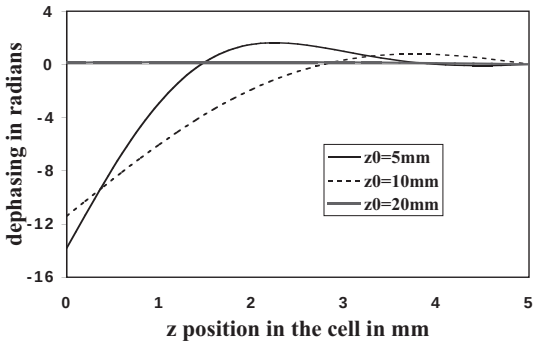

Fig. 4. Dephasing in the gas cell between harmonic radiation and laser-induced polarization at the time of phase-matching for different Rayleigh ranges in the same experimental conditions as in Figure 3; thick grey line: $z_0 = 20$ mm, dotted line: $z_0 = 10$ mm, thin black line: $z_0 = 5$ mm.

at a time when almost perfect phase-matching is achieved at the end of a 5 mm long cell for different Rayleigh ranges. Good phase-matching is represented by a constant phase, equivalent to infinite coherence length $l_{\rm coh} = \pi/\delta k$, where δk is the longitudinal phase gradient. Following Figure 4, if the Rayleigh range is only equal to the cell length, the phase-matching is not homogeneous and the effective length over which the harmonic signal constructively builds up is strongly reduced. If the Rayleigh range becomes much larger than the cell length (4 times), the phase-matching is homogeneous so that the harmonic signal grows all over the medium length. In these conditions, the phase-matching in the loose focusing conditions becomes comparable to that of guided geometry with the advantage of a higher intensity at the time of phase-matching thanks to the contribution of the second quantum path.

3 Imaging and characterization of the focal spot of high harmonics

The focusing of VUV radiation is an hard task due to the lack of easy-to-use optics. That explains why characterization of such focal spots has been done quite recently by Foucault knife-edge technique [15,16]. We present to our knowledge the first image of the focal spot of intense harmonic beam [17].

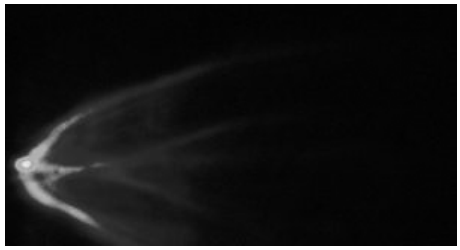

Fig. 5. Image of the focal spot of harmonic, the horizontal size of the frame is 240 μm and the vertical size 128 μm.

3.1 Experimental setup

The harmonic beam produced in the optimized conditions of Section 2 is focused *via* a toroidal mirror with a 100 mm focal length. Compared to multilayer optics [15], this mirror does not induce major time distortion at the focal point. The infrared radiation is totally eliminated by the use of an aluminium filter whose transmission has been experimentally measured to be 0.2. The expected size of the spot is in the micrometer range so that no direct visualization is possible on a CCD camera whose pixel size is much larger. That is why we detect the fluorescence induced in the visible range on a cerium doped YAG crystal by the VUV beam. A magnification of 22 of the imaged size is then obtained by a doublet and the image is recorded by a cooled visible CCD camera: one pixel on the camera represents 0.8 μm in the focal plane. We were able to move the YAG crystal along the propagation axis in order to detect the best focus position.

3.2 Image of the harmonic focus

Figure 5 shows the image of the harmonic focal spot. The global feature of the spot is influenced by aberration effects mainly due to the coma. Limiting these effects implies the use of an iris on the harmonic beam before it is incident on the toroidal mirror. The iris diameter is the compromise between the energy transmission and these aberration effects. We determined an optimum at 2.5 mm leading to 17% transmission.

3.3 Calibration of the focal spot size

The full width at half maximum (FWHM) of the intensity profile is determined by a Gaussian fit and the spot diameter is 3 μm leading to a transverse surface of 7 μm^2. One important thing in order to evaluate the intensity reached at focus is how much energy is contained in this surface compared to the whole energy in the incident beam. The ratio between these two quantities is only 4% in our conditions.

4 Conclusion

All the former considerations can be put together to infer the intensity reached at focus. In theory, the 3.5×10^{10} photons are concentrated on a 7 μm^2 spot so that the intensity should be 3×10^{14} W/cm^2 if the harmonic pulse duration is 10 fs. Moreover, considering [18], we can infer that our one-dimensional loose focusing phase-matching conditions could allow good phase-locking between the high harmonic orders in the spectrum. In these conditions interference in the spectral domain should lead to a train of 7 harmonic bursts of 250-attosecond-duration separated by half the laser period [19]. The maximum intensity reached by one of this burst would then be 2×10^{15} W/cm^2. Following our experimental set-up, additional limiting factors should be taken into account. The aluminium filter transmission (20%) and the platinum reflectivity (40%) are unavoidable parameters, whereas the iris transmission (17%) and the ratio of energy contained in the very central spot (4%) can be most probably improved. The intensity effectively reached in our experimental conditions was 1.4×10^{11} W/cm^2 for 10 fs pulses and 10^{12} W/cm^2 for attosecond pulse trains. This value remains quite low but improving the focusing geometry and limiting the aberration could allow a smaller spot size to be achieved with a larger part of energy inside it. This should allow one to reach a larger intensity in a short-term future and observe new non-linear optic phenomena in this wavelength region.

References

1. M. Schnuerer *et al.*, Phys. Rev. Lett. **83**, 722 (1999)
2. D. Descamps *et al.*, Phys. Rev. A **64**, 031404 (2001)
3. Y. Kobayashi *et al.*, Opt. Lett. **23**, 64 (1998)
4. J.F. Hergott *et al.*, Phys. Rev. A **66**, 021801R (2002)
5. E. Takahashi *et al.*, Phys. Rev. A **66**, 021802R (2002)
6. S. Kazamias *et al.*, Phys. Rev. Lett. (to be published)
7. S. Kazamias *et al.*, Eur. Phys. J. D **21**, 353 (2002)
8. A. L'Huillier *et al.*, Phys. Rev. A **48**, R3433 (1993)
9. E. Constant *et al.*, Phys. Rev. Lett. **82**, 1668 (1999)
10. R.A. Bartels *et al.*, Science **297**, 376 (2002)
11. N.B. Delone, V.P. Krainov, Phys.-Usp. **41**, 469 (1998)
12. M. Lewenstein *et al.*, Phys. Rev. A **52**, 4747 (1995)
13. P. Salières *et al.*, Phys. Rev. Lett. **74**, 3776 (1995)
14. Ph. Balcou *et al.*, Phys. Rev. A **55**, 3204 (1997)
15. L. Le Déroff *et al.*, Opt. Lett. **23**, 1544 (1998)
16. M. Schnuerer *et al.*, Appl. Phys. B **70**, S227 (2000)
17. C. Valentin *et al.*, Opt. Lett. (to be published)
18. M. Gaarde, K. Schafer, Phys. Rev. Lett. **89**, 213901 (2002)
19. P.M. Paul *et al.*, Science **292**, 1689 (2001)